Egypt. J. Chem. **Vol. 68**, No. 11 pp. 363- 375 (2025)

Egyptian Journal of Chemistry

http://ejchem.journals.ekb.eg/

Innovative Graphene Oxide-Folic Acid-MoS_2 Nanocomposite for Targeted Near-Infrared Photothermal Cancer Therapy

Nayer Qenawi[1], Asmaa M. Abd-El aziz[2], Walid Tawfik*[1], Souad A Elfeky*[1]

[1]National Institute of Laser Enhanced Sciences, LAMPA Department, Cairo University, Cairo 12613, Egypt.

[2]Fabrication Technology Research Department, Advanced Technology and New Materials Research Institute, City of Scientific Research and Technological Applications (SRTA-City), Borg El-Arab, Alexandria, Egypt.

Abstract

Cancer, a leading cause of death globally, poses a growing challenge to public health due to increasing population and aging demographics. This study presents a graphene oxide-folic acid-molybdenum disulfide (GO-FA-MoS_2) nanohybrid optimized for targeted, minimally invasive cancer therapy under near-infrared (NIR) light. Its photothermal conversion efficiency and selective targeting of cancer cells are validated through advanced spectroscopic methods, showcasing its potential in clinical applications. By merging the fields of laser physics and nanotechnology, this research introduces a bio-compatible smart nanocomposite that excels in targeted therapeutic efficacy. The nanohybrid synthesis involved an optimized Hummer's method for producing graphene oxide (GO), which was then functionalized with folic acid (FA) to target folate receptor-overexpressing cancer cells, enhancing the specificity of the therapy. Molybdenum disulfide (MoS_2), integrated for its outstanding NIR absorption and photothermal conversion capabilities, was layered with the functionalized GO, creating a potent platform for photothermal cancer therapy. X-ray diffraction (XRD) and Raman spectroscopy validated the nanocomposite's successful synthesis and structural integrity. XRD analysis revealed characteristic peaks indicating the crystalline nature of MoS_2 and the successful integration with graphene oxide. Raman spectroscopy showed distinct shifts in the D and G bands of graphene oxide, suggesting modifications due to the conjugation with MoS_2 and folic acid. Furthermore, UV-visible-NIR spectroscopy illustrated the unique optical properties of the nanohybrid, with significant absorption peaks corresponding to MoS_2 and FA, crucial for effective photothermal action and drug delivery, respectively. These analytical results validate the composite's design and functional attributes, promising a new frontier in targeted and efficient cancer treatment with significant implications for future clinical applications.

Keywords: Graphene Oxide Nanocomposite, Photothermal Therapy, Targeted Drug Delivery, Near-Infrared Spectroscopy, Folic Acid Functionalization.

1. Introduction

Cancer remains one of the main problems that modern medicine must deal with, and it requires new therapeutic interventions because it is very complex, and its symptoms vary widely (Hanahan et al. 2011). Conventional cancer therapies, including surgery, chemotherapy, and radiotherapy, have limitations such as non-specific destruction of normal tissues, the emergence of drug-resistant tumors, and suboptimal treatment efficacy [2]. To solve these issues, alternative therapy approaches must be developed immediately. Phototherapies, such as photothermal therapy (PTT) and photo-dynamic therapy (PDT), have garnered significant scientific attention recently for the treatment of a variety of illnesses, including cancer, because of their special benefits, which include high efficiency and little invasiveness [3]. In the last few years, nanomaterials have emerged as practical tools in combating cancer by providing unique features that allow accurate diagnosis, targeted therapy, and effective treatment methods [4–7]. Graphene oxide (GO), a family member of graphene, is embellished with different functional groups that contain oxygen such as hydroxyl, epoxide, and carboxyl. These functional groups make GO critically considered for cancer treatment because of its unique properties, biocompatibility, high-surface-area, ease of functionalization, and ability to generate heat upon near-infrared light irradiation [8]. For cancer treatment, graphene-based delivery systems can be used to deliver anticancer drugs to targeted sites or used as photothermal agents to kill cancer cells by generating heat. As a two-dimensional (2D) nanomaterial, GO shows remarkable mechanical strength, a high- surface area, and functional groups that facilitate facile surface modification for aimed drug delivery and monitoring in cancer therapy [9]. Therapeutic efficacy can be improved, precise tumor targeting achieved, or treatment responses monitored in real-time through combining targeting ligands, therapeutic agents, or imaging probes at the surface of graphene oxide (GO) and functionalized graphene oxide (FGO) [10]. An example of this approach involves attaching folic acid (FA) to GO to make it more specific for folate receptor-overexpressing cancer cells [11]. Folic acid is a water-soluble vitamin that is essential for nucleotide synthesis and cell division in humans. However, elevated demand and receptor-mediated endocytosis of FA occurs in rapidly dividing cells, including most cancer cells. Its high affinity for folate receptors, which are over-expressed on the surface of many cancer cells, makes FA an ideal ligand for selective tumour targeting [12]. Recently, two-dimensional (2D) transition-metal dichalcogenides (TMDCs) have garnered significant attention across various sectors, particularly in biomedicine, due to their unique physicochemical characteristics. Leveraging their inherent near-

*Corresponding author e-mail: Walid_Tawfik@niles.cu.edu.eg (Walid Tawfik).

Received date: 10 February 2025; Revised date: 17 March 2025; Accepted date: 10 April 2025

DOI: 10.21608/EJCHEM.2025.358734.11274

infrared absorption and large specific surface area, considerable research is being directed towards developing a multifunctional nanoplatform using 2D TMDCs. This platform aims to combine photothermal therapy (PTT) with other therapeutic modalities, facilitating the advancement of 2D TMDC-enabled combination therapies that demonstrate outstanding efficacy in tumour treatment [13]. The transition metal disulphide molybdenum disulphide (MoS_2) resembles graphene in its layered structure. Unique characteristics of MoS_2 include its high surface area, high photothermal conversion capacity, superior biocompatibility, and effectiveness in drug delivery applications [14]. Specifically, 2D MoS_2 with outstanding bio-compatibility and effective bio-degradability can be utilized as extraordinary nano-templates to hybridize their performing elements for highly efficient cancer theranostics [15]. Furthermore, the problem of low NIR absorption in biological tissues is successfully addressed by MoS_2 nanosheets, which stand out for their exceptional absorption and effective photothermal conversion in the near-infra-red (NIR) range. MoS_2 nanosheets' exceptional photothermal conversion efficiency and high biocompatibility suit the needs for NIR conversion agents in tumour photothermal therapy (PTT). Phototherapies, such as photo-dynamic therapy (PDT) and photothermal therapy (PTT), have garnered significant scientific attention recently for the treatment of a variety of illnesses, including cancer, because of their special benefits, which include high efficacy and low invasiveness [16]. The electronic properties of MoS_2 have been shown to rely on the nature of its dimensionality, where a monolayer form is characterized with a direct bandgap of about 1.8 eV, while that of the bulk display an indirect bandgap is around 1.2 eV. The presence of a direct bandgap in monolayer MoS_2 provides additionally a big advantage in the absorption of photons in the visible and near-infrared region. If photons of enough energy collide with MoS_2, they may excite the electrons from the valence band to the conduction band and subsequently produce the electron-hole pairs. Such excited carriers lose energy quite quickly through non-radiative processes with this energy being transferred to the lattice in the form of vibration or phonons. This is essentially the photothermal effect, based on how electron-phonon coupling raises the local temperature. A highly efficient photothermal mechanism of MoS_2 involves light absorption, leading to electrons excited from the valence band to the conduction band and the subsequent generation of electron-hole pairs. Upon such excitation, the carriers rapidly undergo non-radiative recombination, transferring energy to the lattice via electron-phonon composure, leading to localized heating. Since its direct bandgap allows efficient photon absorption and subsequent energy conversion into heat, this process is highly effective in monolayer MoS_2 [17, 18]. PTT is recognized for its low invasiveness and high selectivity in targeting cancer cells [19, 20]. PTT and PDT use photothermal agents or photosensitizers to destroy cancer cells with a single light source. In order to produce local hyperthermia, which kills cancer cells, PTT needs photothermal materials to transform the energy of received photons into heat. In PDT, reactive oxygen species (ROS) produced by photosensitizers under light irradiation kill cancer cells [21]. Despite these advantages, PTT and PDT monotherapies have several drawbacks. The important therapeutic problem in single photodynamic treatment is that tissue oxygen depletion exacerbates local-hypoxia, reducing the efficiency of ROS generation. This problem, in return, attenuates PDT efficiency. PDT and PTT together can improve blood flow to the tumour location, which raises the oxygen content. Additionally, the majority of photothermal agents are made of inorganic chemicals, which may be harmful over the long term and have poor biodegradability. Graphene-based nanomaterials have emerged as interesting candidates for photothermal applications because of their unique 2D structure and excellent photothermal conversion efficiency, biocompatibility, and low toxicity [22]. To improve drug delivery efficacy, in this study, an attempt has been made to design a folic acid-conjugated graphene oxide-molybdenum disulfide nanocomposite (GO-FA-MoS_2). This study advances photothermal therapy by integrating MoS2's superior NIR properties with graphene oxide's functional versatility for improved cancer targeting. Graphene oxide (GO) is a versatile biocompatible 2D nanomaterial that can easily be combined with other nanomaterials to form nanocomposites. MoS_2 nanosheets were prepared using a liquid exfoliation method and were subsequently composited with GO. Folic acid (FA) was then conjugated to the surface of GO-MoS_2 nanocomposite and the functionalization of this GO-FA-MoS_2 nanocomposite by folic acid provides good hydrophilicity by functionalizing the surface of the graphene oxide with polar functional groups like carboxyl and hydroxyl groups. This addition helps to improve the interactions of the nanocomposite with water molecules, thus enhancing its dispersibility in aqueous media [7]. Photothermal therapy, as a treatment for cancer, is facing rapid innovations using photothermal agents for tumor ablation, utilizing the basic principle of converting light energy into localized heat. Many types of materials have shown a very high ability of photothermal performance, including, but not limited to, gold nanorods, CNTs, and black phosphorus. Gold nanorods have been well-equipped with localized surface plasmon resonance (LSPR) to achieve efficient light absorption specifically in the NIR region but often are susceptible to toxicity due to the concentrated amounts required. CNTs absorb and convert NIR energy into heat very effectively, yet their cytotoxicity and long-term accumulation in biological systems are a growing concern. Black phosphorus shows a different set of problems owing to its instability during oxidation, therefore limiting its use in biology, however it also shows aspects of desirable NIR performance since it absorbs from visible light to the NIR. Meanwhile, GO-FA-MoS_2 nanocomposite involves graphene oxide (GO), folic acid (FA), and molybdenum disulfide (MoS_2), which utilizes the direct bandgap of MoS_2 for effective photon absorption and photothermal conversion. This mixture possesses comparable or better photothermal conversion kinetics than that of gold nanorods or CNTs while having good biocompatibility via GO stability and selective targeting imposed by FA functionalization, thus being an interesting candidate for targeted cancer treatment like the previous studies as mentioned in Table 1. [18, 23–26]. The GO-FA-MoS_2 nanocomposite combines the photothermal efficiency of MoS_2 (~40% conversion efficiency, as reported by [27]) with the biocompatibility of GO and targeting capability of FA, offering a balanced alternative to conventional agents.The synthesized nanocomposite GO-FA-MoS_2 was characterized using various bio-physical techniques such as UV-visible spectroscopy, Fourier transform infra-red spectroscopy, Raman spectroscopy, and transmission electron microscopy.

Table1. Quantitative comparison of different photothermal agents

Material	Photothermal Efficiency	Biocompatibility	Key Limitations
Gold Nanorods	High (LSPR-dependent)	Moderate	Toxicity at high concentrations
Carbon Nanotubes	High	Low	Long-term bioaccumulation risks
Black Phosphorus	High	Moderate	Rapid oxidation in aqueous media
GO-FA-MoS_2	Comparable/High	High	Stable, targeted delivery

2. Experimental (Materials and Methods)

2.1. Materials

Graphite powder (< 20µm), Sulfuric acid (H_2SO_4), hydrochloric acid (HCl), potassium permanganate ($KMnO_4$), and hydrogen peroxide (H_2O_2) were purchased from Sigma-Aldrich. Also procured were folic acid, sodium monochloroacetate, sodium hydrogen carbonate, sodium nitrite, sulphanilic acid, tannic acid, molybdenum disulfide powder, N-Hydroxy succinimide (NHS), 1-(3-Dimethyl-aminopropyl)-3-Ethyl Carbodiimide Hydrochloride (EDC) and other reagents utilized in the synthesis process. The materials were obtained under strict quality control to ensure their suitability for the preparation of the nanocomposite [28, 29].

2.2. Methods

2.2.1. Synthesis of graphene oxide GO

As seen in **Fig. 1a**, graphene oxide (GO) was created utilizing an enhanced Hummer process for environmentally benign use, obviating the need for $NaNo_3$ and the development of harmful gases ($NO_2/N2O_4$). Briefly, in order to keep the temperature below 20 °C, concentrated H_2SO_4 (23 mL, 98%) and graphite powder (1.0 g) were first combined while being vigorously stirred in an ice bath. Potassium permanganate $KMnO_4$ (3.0 g) was then added gradually. After that, the mixture was transferred to an oil bath set at 40°C and constantly swirled for around half an hour. The mixture was stirred for 15 minutes at 95 °C after 50 mL of water was added. The solution's colour changed from dark brown to yellow when (50 mL) of distilled water was added and then H_2O_2 (10 mL, 30%) was gradually added. To get rid of the metal ions, the solution was filtered and rinsed with a (1:10) HCl aqueous solution (250 mL). Until the pH of the solution was neutral, the precipitate was rinsed with distilled water. Finally, the aqueous dispersion of graphene oxide was sonicated using an ultrasonic probe for 60 minutes [30].

2.2.2. Conjugation of graphene oxide with folic acid

As shown in **Fig. 1b** begin by adding the prepared graphene oxide (100 mL, 1 mg/mL), followed by NaOH (5 g) and sodium monochloroacetate ($ClCH_2COONa$, 5 g). Sonicate this mixture for two hours, then neutralize the resultant product (GO-COOH) using diluted HCl. Next, use centrifugation to wash the neutralised product five times with distilled water. Next, dialyze the GO-COOH suspension against distilled water for over two days to eliminate ions.

Subsequently, dissolve sulfanilic acid (200 mg) and sodium nitrite (80 mg) in 20 mL of (0.25% NaOH). In an ice bath, slowly add this solution drop by drop to (26 mL of 0.1 N) HCl. Leave the carboxylated graphene oxide (GO-COOH) dispersion in an ice bath, introduce the diazonium salt solution to the dispersion, and stir for two hours. After another two days of dialysis against double-distilled (DD) water, store the resulting sulfonated GO ($GOSO_3H$) at 4 °C.

Finally, conjugate the GO-SO_3H with folic acid (FA) following a previously established protocol [31]. First, activate a 100 mg dispersion of prepared (GO-SO_3H) with an EDC/NHS solution, followed by ultrasonication treatment for two hours. Next, add 20 mL of a 0.5% folic acid (FA) solution to create a mixture, and allow this to react at room temperature for 12 hours. Dialyze the mixture first against a sodium-bicarbonate solution (pH --- 8.0) for two days and then against double-distilled (DD) water for one day to remove unreacted materials [32].

2.2.3. Synthesis of nano TMD's (MoS_2)

First, prepare a 60 mL (aqueous solution) with tannic acid (60 mg) and MoS_2 powder (120 mg), and then sonicate the final suspensions for two hours. To isolate the exfoliated MoS_2 nanosheets, centrifuge the mixture at 6000 rpm for 15 minutes and collect the supernatant containing the MoS_2 nanosheets, removing any unexfoliated MoS_2 [33].

2.2.4. Preparation of GO-FA-MoS_2

First, dissolve the prepared GO-FA (100 mg) in 50 mL of distilled water and subject it to bath sonication for 15 minutes. This step adds the aqueous GO-FA suspension to a 50 mL aqueous dispersion of previously prepared nano MoS_2. Stir the resultant mixture overnight under ambient conditions. Finally, freeze-dry the resulting GO-FA-MoS_2 as shown in **Fig. 1c**.

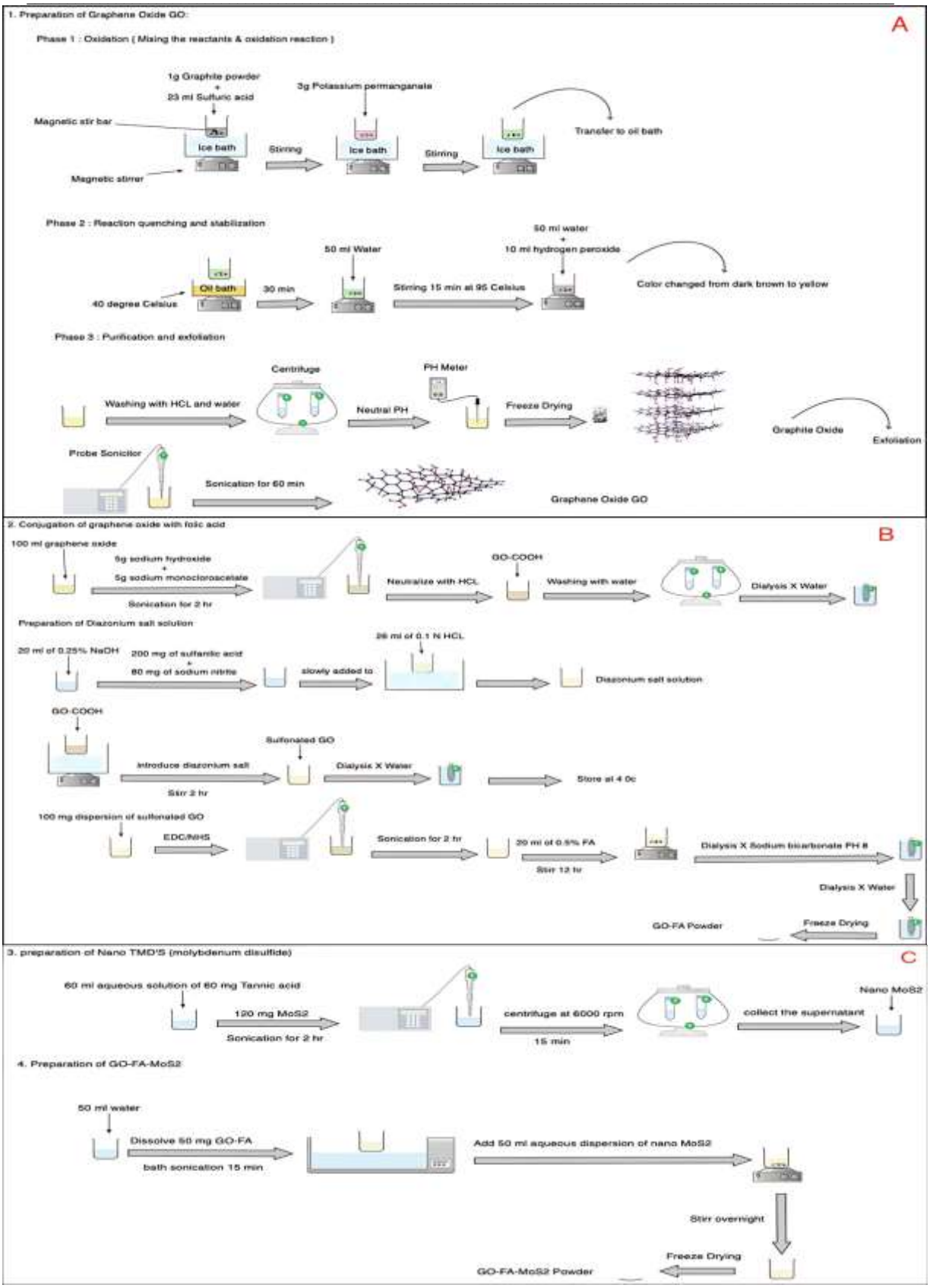

Fig. 1: A) Preparation of graphene oxide, B) Conjugation of GO With FA, and C) Preparation of MoS_2 and GO-FA-MoS_2 composite.

2.3. Characterization Techniques

A range of spectroscopic methods were used to examine the phase structure and composition of the synthesized products. The D8-Discover X-ray diffractometer (Bruker, UK) with Cu-Kα radiation (λ = 1.54060 Å) was used to perform X-ray diffraction (XRD) measurements at 40 kV and 30 mA settings, covering a 2θ range from 5 to 80°. A Lab RAM HR Evolution Raman spectrometer (HORIBA Scientific, France) equipped with a 532 nm laser source for excitation was used to record the Raman spectra. The MoS_2/GO composites' Fourier transform infrared (FTIR) spectra were acquired in the optical range of 4000–500 cm^{-1} using a Bruker FTIR spectrometer (Bruker Optics Ltd, Coventry, UK). Quartz cuvettes with a 1 cm route length were examined for UV-visible absorption spectra using a Thermo 600 UV-Vis spectrophotometer. Using a Shimadzu TGA-50 thermogravimetric analysis (TGA) device, the thermal stability of the synthesised nanocomposite was evaluated. Weight loss as a function of temperature was assessed using an analysis of about 5 mg of sample. Imaging, crystal structure determination, and elemental analysis (both qualitative and semi-quantitative) were performed using a high----resolution transmission electron microscope (HR-TEM, JEOL-- 2100 Plus, Japan).

3. Results and discussion

The suspensions were characterized using UV-visible spectrophotometry, FTIR, AFM, TGA, and XRD analysis. The GO-FA-MoS_2 nanocomposite was synthesized by linking MoS_2 with GO-FA. GO-FA was synthesized by conjugation of GO with FA and the combination was done using carbodiimide chemistry. To achieve the conjugation, the carboxyl groups on the surface of GO were first activated with (EDC) and (NHS) to create an active ester intermediate. Then, folic acid was added, and the amine groups could react with the activated GO, allowing the formation of stable amide bonds. Charge-transfer processes between GO and MoS_2 play a critical role in regulating the electronic and optical properties of the nanocomposite. The interactions between the two materials lead to a higher charge distribution and mobility, which improves the conductivity of the composite. At the same time, the charge transfer process determines the changes in the absorption spectrum, thereby enhancing the ability of the nanocomposite to absorb light specifically in the near-infrared region. Photothermal applications especially benefit from such modifications, with efficient light absorption and conversion to heat being of great importance. Notably, generation of charge transfer between GO and MoS_2 synergistically boosts not only the electronic operation of the material but also its photothermal efficiency, thus making it a potential candidate for targeted cancer therapy and other photothermal applications [34, 35]. GO-FA-MoS_2 was synthesized by linking MoS_2 and FA-MoS_2 with GO, where FA was grafted onto GO through carbamate. Characterization of GO, MoS_2, and GO-FA-MoS_2 nanocomposite included UV-visible spectrophotometry, FTIR, TEM imaging, XRD pattern, TGA, zeta potential measurement, and DLS analysis [2].

A. XRD analysis

The graphene oxide (GO), MoS_2, and MoS_2/GO/FA composites were identified by XRD in terms of their composition and crystallographic structure. As illustrated in **Fig.2**, the graphene oxide shows a wide diffraction peak that is at 2θ=9.88° with the spacing between plane d_{001} is 8.94 A°. Two peaks show at 2θ= 21.33° and 23.52°, which correspond to lattice spacings of 4.16 A° and 3.77 A°, respectively. This suggests that the nanographene oxide may consist of defects, folding, sp., sp^2, and sp^3 hybridization carbon structures, as well as randomly orientated graphitic plates. The constricted lattice space (002) plane of graphitic carbon has a minimally intense peak at 2θ= 26.14°. This lattice space contraction is seen in the carbon structure's nanoscale regime. [36]. **Fig. 2** displays a prominent diffraction peak at 2θ= 14.31°, with additional peaks at 2θ= 29.40°, 32.68°, 35.88°, and 39.57°, corresponding to the lattice planes (002), (004), (100), (102), and (103), of crystalline MoS_2, respectively [37]. It is noteworthy that the addition of graphene to the complex results in a decrease in the intensity of the MoS_2 diffraction peak, suggesting that, up to a certain point, graphene dominates the formation of MoS_2 crystals along the (002) plane in the composite. [38]. By distinguishing, MoS_2/GO/FA composites indicate reduced peaks, indicating that the crystallite size and the number of layers along the axis are much lesser than those of MoS_2 nanosheets [39].

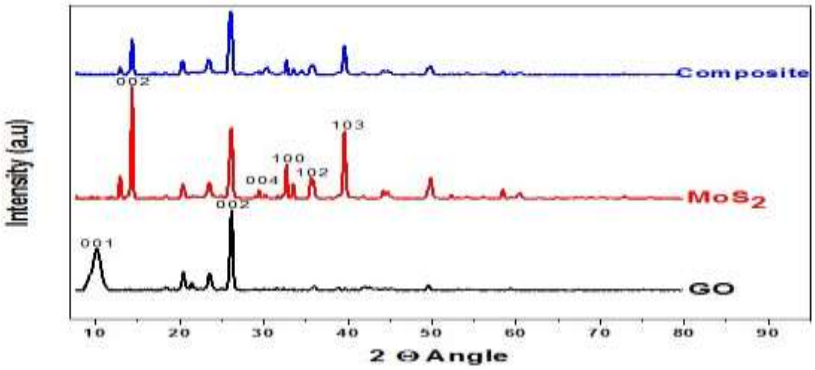

Fig. 2: XRD of graphene oxide, MoS_2, and (GO-FA-MoS_2) composite.

B. Raman spectra analysis

The Raman spectrum of nanographene oxide is displayed in **Fig. 3** and includes the characteristic D-band at 1349 cm^{-1}, which represents breathing modes or rings of K-point phonons of A_{1g} symmetry, and the band known as G-band at 1581 cm^{-1}, which discloses defects in the crystalline structure of graphene and gets generated by the first order scattering of E_{2g} phonons of sp^2 crossed carbon atom. For nanographene oxide, the (D to G) band's intensity ratio (ID/IG) was 1.04. The 2D band of (NGO) found at 2702 cm^{-1} is due to the overtone of transverse optical phonons around the K point [40]. The strength, frequency, and width of the peaks as well as the Raman features are significantly influenced by the number of layers. MoS_2's Raman spectrum shows two strong peaks at 375 cm^{-1} and 402 cm^{-1}, which correspond to the S atoms' in-plane (E^1_{2g}) and out-of-plane (A_{1g}) vibrational modes, respectively [41]. Both the E^1_{2g} and A_{1g} bands redshift as GO is conjugated into MoS_2, indicating that the MoS_2 layer becomes more n-doped (i.e., the electron concentration increases). The outcome further demonstrates that GO has been successfully incorporated into MoS_2 [42].

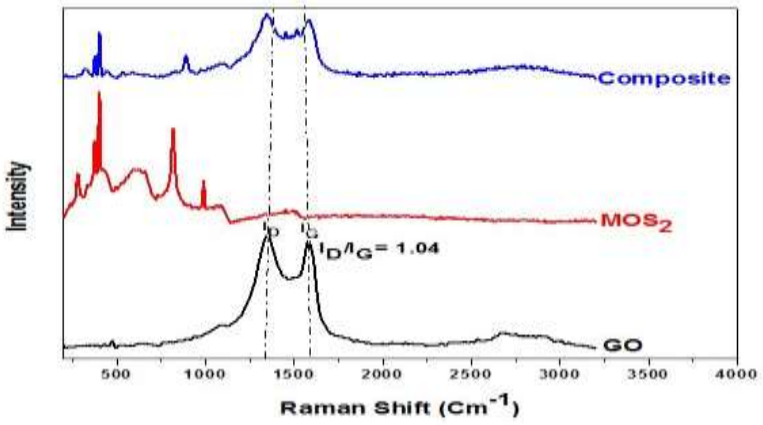

Fig. 3: Raman analysis of GO, MoS_2, and (GO-FA-MoS_2) composite.

C. UV-VISIBLE Spectroscopy

The UV absorbance of graphene oxide (GO), which is commonly displayed in **Fig. 4A** at about 230 nm, is frequently taken into consideration [43]. A characteristic absorption of folic acid was obtained at 226 nm, 282 nm, and 346 nm [44]. As seen from the UV/Vis spectra of (GO-FA), a peak at 230 nm disappears, whereas a new peak at 264 nm develops, which may be because of the linking of FA with NGO and the shift in absorption peaks compared to pristine GO further supports the successful conjugation of FA [45]. The TA-stabilized MoS_2 dispersions, as explored in **Fig. 4B**, reveal two absorption peaks at 620 nm (B-exciton peak of MoS_2) and 686 nm (A-exciton peak of MoS_2) in the absorption spectra UV-vis band [33]. Following the GO-FA-MoS_2 composite's production, the observed dispersions' UV–vis spectra were measured and displayed in **Fig. 4A**. The UV-vis spectrum of GO–FA–MoS_2 also shows the peak at 260 nm attributed to the FA following the filling of the GO–FA with MoS_2. These findings all demonstrate that FA molecules are successfully conjugated onto GO. A redshift into the longer wavelength area on GO–the current investigation confirms FA-MoS2. When GO–FA–MoS_2 is being prepared, the remaining unpaired π electrons ought to form a bond with free (Mo) atoms as soon as possible [46].

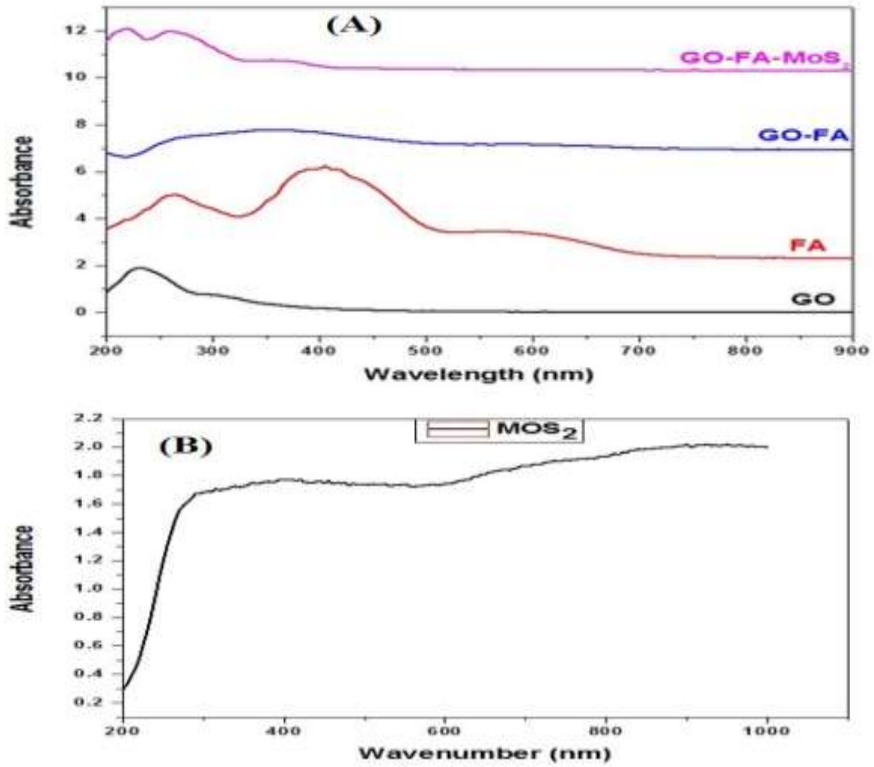

Fig. 4: UV-Vis absorption of (A): (GO, FA, GO-FA, GO-FA-MoS_2), and (B): MoS_2.

D. FTIR spectroscopy

The FTIR spectrum of graphene oxide (GO) in Figure 5 shows a large peak at 3423 cm^{-1} in the high-frequency region, which is ascribed to the O-H bond stretching mode and indicates that graphene oxide contains hydroxyl groups. This band is attributed to the carboxyl group (C=O) at 1728 cm^{-1}. Water molecules adsorbed on graphene oxide exhibit stretching and bending vibrations of their (OH) groups, as evidenced by a strong peak at 1626 cm^{-1}. The peak at 1225 cm^{-1} shows (C-O-C) stretching, whereas the peak at 1384 cm^{-1} originates from the (C-O-H) group. The (C-O) group's vibrational mode is represented by the peak at 1056 cm^{-1} [47]. A new peak at 1625 cm^{-1} in the FTIR spectra of GO-FA indicates the existence of (C-O-N-H) groups. These additional peaks indicate the successful covalent bonding of FA to the GO surface. (Mo–S) vibrations are responsible for the peak at 600 cm^{-1} of the GO-FA-MoS_2 final composite, while (Mo-O) stretching vibrations are responsible for the peak at 830 cm^{-1} [48]. (C=C) stretching vibrations are linked to the peak at 1670 cm^{-1}, while (C–O) stretching vibrations are detected at 1300 cm^{-1} [49].

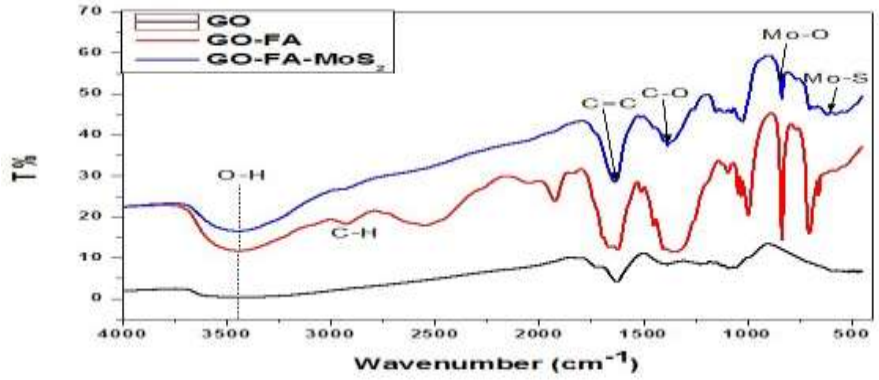

Fig. 5: FTIR spectra for the prepared nanoparticles (GO, GO-FA, and GO-FA-MoS_2).

E. Thermal analysis

The TGA is frequently used to analyze the decomposition properties of various biomaterials [50]. The thermal stabilities of (GO, MoS_2, and the GO-FA-MoS_2 composite) were studied by thermo-gravimetric analyses (TGA) (**Fig. 6**). The TGA curve of graphene oxide (GO) is shown in **Fig. 6a**. It is evident that the graph also shows two stages of mass loss. The initial mass loss is a result of moisture removal. A mass loss of 12.14% occurred during the first stage, which occurred between 50 and 71.43 °C. The second mass loss, 32.62%, has a steeper slope because graphene oxide breaks down at temperatures between 71.43 and 241.81 °C to produce volatile water, carbon dioxide, and char [51]. MoS_2 exhibits a five-stage weight loss in **Fig. 6b.** The evaporation of surface-absorbed water molecules is responsible for the initial mass loss of 4.5% at 75.87 °C. The second mass loss of 28.12% at 177.91 °C corresponds to the material continuing to lose small amounts of water or sulfur-containing species weakly bound to the surface. The third mass loss of 34.89% among (177.97 – 474) °C, a fairly large mass loss takes place, generally because oxidation of molybdenum disulfide (MoS_2) to molybdenum trioxide (MoO_3) and sulfur dioxide (SO_2). And between (474- 876) °C, the mass loss can be attributed to oxidation or decomposition of the remaining sulfur species. Finally, between (876.85-989) °C, this period is the completing stage of the TGA, at which any remaining trace sulfur, sulfur-containing gas, and residues of MoS_2 would have been removed [52]. Comparatively, the stability of the GO-FA-MoS_2 composite is higher than that of GO but lower than MoS_2 as shown in **Fig. 6c**.

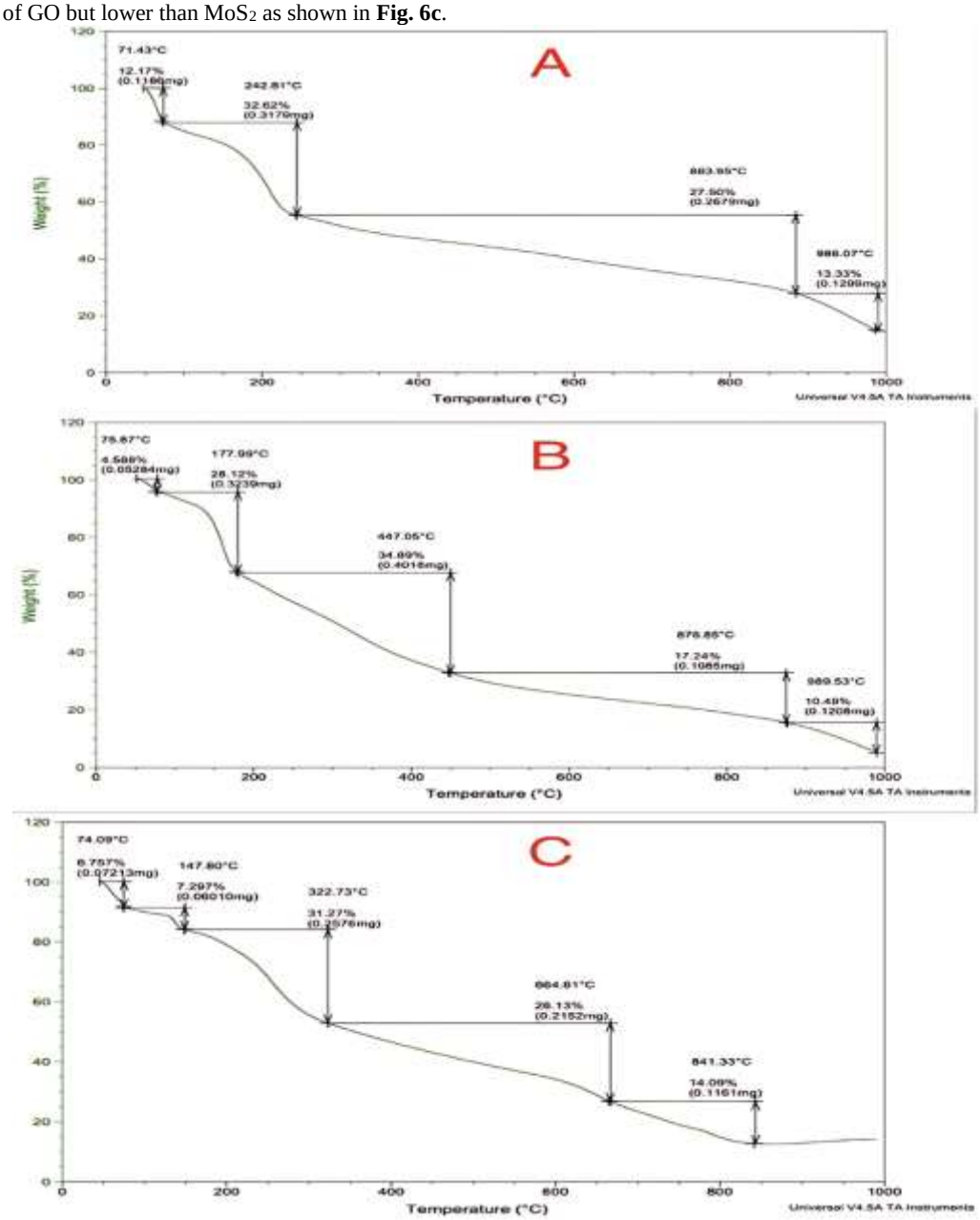

Fig. 6: TGA curves of a) GO, b) MoS_2, and c) GO-FA-MoS_2.

F. Transmission electron microscopy

High---resolution transmission electron microscopy (HR-TEM) was used to characterize the morphological structure of GO and GO-FA-MoS_2, which is shown in (**Fig. 7)**. **Fig. 7a** explores that GO is essentially transparent. However, the GO's surface frequently has varying brightness due to the elastic corrugations and the scrolled or folded edges [53]. TEM micrographs show that the molybdenum disulfide nanoparticles are deposited on graphene oxide sheets. MoS_2 nanoparticles are visible in this picture as dark spots with a diameter of 37–71 nm on a lighter-colored substrate, which represents the planar graphene oxide sheet, as shown in **Fig. 7b** and **Fig. 7c**. **Fig. 7D** represents an HRTEM micrograph of GO sheets and clearly shows graphene's lattice fringes. This pattern gives additional information about the IFFT interplanar spacing, which is equal to (0.244 ± 0.04) nm. The graphene oxide SAED pattern is displayed in **Fig. 7E**. There are distinct diffraction spots visible in the diffraction patterns. Under the circumstances employed here, these are traits of crystalline organization and favored crystalline orientation over a length scale of the electron beam's coherence length, which is a few nm [54]. For comparison, the interplanar distance d001 of the graphite layers was measured to be about 8.99 Å, as shown in **Fig. 2**, and this data is in good accordance with the XRD.

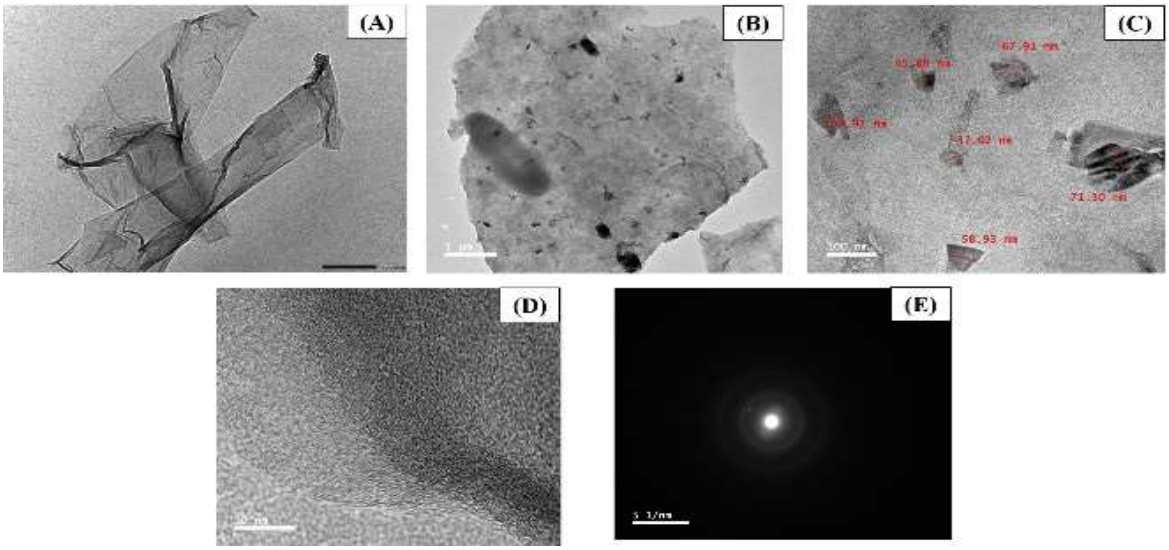

Fig. 7: TEM Images of the prepared materials (a) GO, b) GO-FA-MoS_2 and C) represent GO-FA-MoS_2 size, D) HR-TEM image of GO, E) Selected Area Electron Diffraction Pattern (SAED) of GO.

G. Energy dispersive X-ray analysis

EDX analysis was conducted to determine the elemental composition of the synthesized GO-FA-MoS_2 nanocomposite sample. As shown in **Fig. 8**, four signals of the elemental composition of C, O, Mo, and S elements were detected from the synthesized GO-FA-MoS_2 sample with weight percentages of 48.75, 37.29, 8.07, and 5.89, respectively.

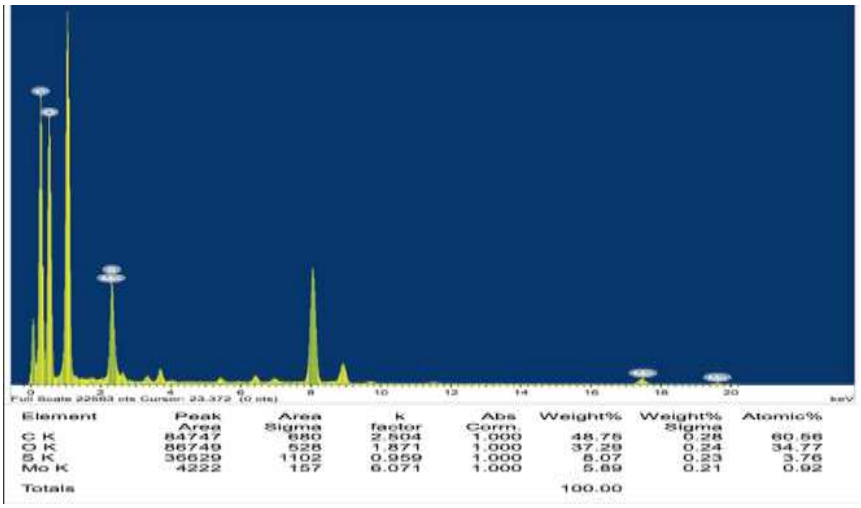

Element	Peak Area	Area Sigma	k factor	Abs Corrn.	Weight%	Weight% Sigma	Atomic%
C K	84747	880	2.504	1.000	48.75	0.28	60.56
O K	86749	528	1.871	1.000	37.29	0.24	34.77
S K	36629	1102	0.959	1.000	8.07	0.23	3.76
Mo K	4222	157	6.071	1.000	5.89	0.21	0.92
Totals					100.00		

Fig. 8: EDX Spectrum of GO-FA-MoS_2.

4. Conclusion

In conclusion, synthesizing and characterizing the graphene oxide-folic acid-molybdenum disulfide (GO-FA-MoS_2) nanohybrid is a significant advancement in cancer therapy. This multifunctional nanocomposite demonstrates exceptional potential for precise cancer treatment under near-infrared (NIR) light. The successful synthesis involved optimizing Hummer's method and folic acid functionalization to enhance targeting specificity. Molybdenum disulfide (MoS_2) integration conferred remarkable NIR absorption and photothermal conversion, crucial for effective therapy. Characterization studies confirmed the nanohybrid's structural integrity and functional attributes, validating its design and performance. In future studies, the cytotoxicity of GO-FA-MoS_2 towards cancer cells under NIR light will be investigated. This research establishes a foundation for developing multifunctional nanocomposites for targeted cancer therapy. The GO-FA-MoS_2 nanocomposite shows great promise for clinical purposes in drug delivery and tumor imaging tasks. After further optimization and expansive preclinical tests, it can be considered a reliable tool for cancer treatment and diagnostics. However, for its successful transition into real-world use, it is necessary to consider challenges concerning scalability, toxicity, and potential to get regulatory clearance. Future studies will focus on in vivo assessments and enhancing biocompatibility to transition from preclinical validation to clinical application. These innovations synergistically integrate nanotechnology and laser physics, offering paving the way for personalized and effective cancer treatment strategies. This study aligns with the United Nations Sustainable Development Goal (SDG) 3, which aims to ensure healthy lives and promote well-being for all at all ages. Specifically, our work on developing advanced nanomaterials for cancer therapy, including the GO-FA-MoS_2 nanocomposite for targeted drug delivery and photothermal therapy, contributes to improving cancer treatment options. By enhancing the efficacy and targeting capability of therapies, this research has the potential to improve health outcomes and reduce inequalities in healthcare access, supporting the achievement of SDG 3.

Declarations

Ethical Approval

This work does not apply to investigations involving humans or animals.

Competing interests

I certify that the authors have no conflicting interests that might be seen as influencing the findings and/or debate presented in this work.

Conflicts of Interest

No conflicts of interest are disclosed by the writers.

Authors' contributions

Each author has made an equal contribution to the manuscript.

Funding

This research received funding from Science, Technology & Innovation Funding Authority (STDF) under grant number 45893.

Acknowledgment

This paper is based upon work supported by the Science, Technology & Innovation Funding Authority (STDF) under grant number 45893.

References and Bibliography

[1] Hanahan, D.; Weinberg, R. A. Hallmarks of Cancer: The next Generation. *Cell*. March 4, 2011, pp 646–674. https://doi.org/10.1016/j.cell.2011.02.013.

[2] Thapa, R. K.; Choi, J. Y.; Poudel, B. K.; Choi, H. G.; Yong, C. S.; Kim, J. O. Receptor-Targeted, Drug-Loaded, Functionalized Graphene Oxides for Chemotherapy and Photothermal Therapy. *Int J Nanomedicine*, 2016, *11*, 2799–2813. https://doi.org/10.2147/IJN.S105401.

[3] Guo, S.; Song, Z.; Ji, D. K.; Reina, G.; Fauny, J. D.; Nishina, Y.; Ménard-Moyon, C.; Bianco, A. Combined Photothermal and Photodynamic Therapy for Cancer Treatment Using a Multifunctional Graphene Oxide. *Pharmaceutics*, 2022, *14* (7). https://doi.org/10.3390/pharmaceutics14071365.

[4] Peer, D.; Karp, J. M.; Hong, S.; Farokhzad, O. C.; Margalit, R.; Langer, R. Nanocarriers as an Emerging Platform for Cancer Therapy. *Nat Nanotechnol*, 2007, *2* (12), 751–760. https://doi.org/10.1038/nnano.2007.387.

[5] Gamal, H.; Tawfik, W.; El-Sayyad, H. I.; Emam, A. N.; Fahmy, H. M.; El-Ghaweet, H. A. A New Vision of Photothermal Therapy Assisted with Gold Nanorods for the Treatment of Mammary Cancers in Adult Female Rats. *Nanoscale Adv*, 2023, *6* (1), 170–187. https://doi.org/10.1039/d3na00595j.

[6] Gamal, H.; Tawfik, W.; El-Sayyad, H. H.; Fahmy, H. M.; Emam, A. N.; El-Ghaweet, H. A. Efficacy of Polyvinylpyrrolidone-Capped Gold Nanorods against 7,12 Dimethylbenz(a)Anthracene-Induced Oviduct and Endometrial Cancers in Albino Rats. *Egyptian Journal of Basic and Applied Sciences*, 2023, *10* (1), 274–289. https://doi.org/10.1080/2314808X.2023.2185615.

[7] Elfeky, S.; Qenawi, N.; Tawfik, Prof. W.; Loutfy, S.; Subash, T. Utilization of Nanographene Oxide-Folic Acid-Metal Chalcogen in Cancer Theranostics. *NanoWorld J*, 2024, *9*, 206–214. https://doi.org/10.17756/nwj.2023-s5-041.

[8] Zhang, Y.; Nayak, T. R.; Hong, H.; Cai, W. Graphene: A Versatile Nanoplatform for Biomedical Applications. *Nanoscale*, 2012, *4* (13), 3833–3842. https://doi.org/10.1039/C2NR31040F.

[9] Liu, Z.; Robinson, J. T.; Sun, X.; Dai, H. PEGylated Nanographene Oxide for Delivery of Water-Insoluble Cancer Drugs. *J Am Chem Soc*, 2008, *130* (33), 10876–10877. https://doi.org/10.1021/ja803688x.

[10] Yang, K.; Feng, L.; Shi, X.; Liu, Z. Nano-Graphene in Biomedicine: Theranostic Applications. *Chem. Soc. Rev.*, 2013, *42* (2), 530–547. https://doi.org/10.1039/C2CS35342C.

[11] Zhang, L.; Xia, J.; Zhao, Q.; Liu, L.; Zhang, Z. Functional Graphene Oxide as a Nanocarrier for Controlled Loading and Targeted Delivery of Mixed Anticancer Drugs. *Small*, 2010, *6* (4), 537–544. https://doi.org/10.1002/smll.200901680.

[12] Lu, Y.; Low, P. S. Folate-Mediated Delivery of Macromolecular Anticancer Therapeutic Agents. *Adv Drug Deliv Rev*, 2012, *64*, 342–352. https://doi.org/https://doi.org/10.1016/j.addr.2012.09.020.

[13] Gong, L.; Yan, L.; Zhou, R.; Xie, J.; Wu, W.; Gu, Z. Two-Dimensional Transition Metal Dichalcogenide Nanomaterials for Combination Cancer Therapy. *J. Mater. Chem. B*, 2017, *5* (10), 1873–1895. https://doi.org/10.1039/C7TB00195A.

[14] Samy, O.; Zeng, S.; Birowosuto, M. D.; El Moutaouakil, A. A Review on MoS2 Properties, Synthesis, Sensing Applications and Challenges. *Crystals (Basel)*, 2021, *11* (4). https://doi.org/10.3390/cryst11040355.

[15] Li, X.; Kong, L.; Hu, W.; Zhang, C.; Pich, A.; Shi, X.; Wang, X.; Xing, L. Safe and Efficient 2D Molybdenum Disulfide Platform for Cooperative Imaging-Guided Photothermal-Selective Chemotherapy: A Preclinical Study. *J Adv Res*, 2022, *37*, 255–266. https://doi.org/10.1016/j.jare.2021.08.004.

[16] Gurunathan, S.; Han, J. W.; Park, J. H.; Kim, E.; Choi, Y. J.; Kwon, D. N.; Kim, J. H. Reduced Graphene Oxide-Silver Nanoparticle Nanocomposite: A Potential Anticancer Nanotherapy. *Int J Nanomedicine*, 2015, *10*, 6257–6276. https://doi.org/10.2147/IJN.S92449.

[17] Iqbal, S.; Fakhar-e-Alam, M.; Atif, M.; Ahmed, N.; Aqrab-ul-Ahmad; Amin, N.; Alghamdi, R. A.; Hanif, A.; Farooq, W. A. Empirical Modeling of Zn/ZnO Nanoparticles Decorated/Conjugated with Fotolon (Chlorine E6) Based Photodynamic Therapy towards Liver Cancer Treatment. *Micromachines (Basel)*, 2019, *10* (1). https://doi.org/10.3390/mi10010060.

[18] Jassim, J.; Al-samak, M.; Younes, W.; Kisov, H. Near-Infrared Plasmonic Random Laser Emission Employing Gold Nanorods and LDS-821 Dye. *Plasmonics*, 2025, 1–8. https://doi.org/10.1007/s11468-025-02765-3.

[19] Lu, J.; Chen, M.; Dong, L.; Cai, L.; Zhao, M.; Wang, Q.; Li, J. Molybdenum Disulfide Nanosheets: From Exfoliation Preparation to Biosensing and Cancer Therapy Applications. *Colloids Surf B Biointerfaces*, 2020, *194*, 111162. https://doi.org/https://doi.org/10.1016/j.colsurfb.2020.111162.

[20] Elfeky, S.; Qenawi, N. Nanoformulations in Cancer Theranostics; 2024. https://doi.org/10.1007/16833_2024_446.

[21] Xu, C.; Pu, K. Second Near-Infrared Photothermal Materials for Combinational Nanotheranostics. *Chem. Soc. Rev.*, 2021, *50* (2), 1111–1137. https://doi.org/10.1039/D0CS00664E.

[22] Li, Z.; Lei, H.; Kan, A.; Xie, H.; Yu, W. Photothermal Applications Based on Graphene and Its Derivatives: A State-of-the-Art Review. *Energy*, 2020, *216*, 119262. https://doi.org/10.1016/j.energy.2020.119262.

[23] Ahmed, N.; Khalil, Z.; Farooq, Z.; Khizar-Ul-Haq, N.; Shahida, S.; Ramiza, N.; Ahmad, P.; Qadir, K. W.; Khan, R.; Zafar, Q. Structural, Optical, and Magnetic Properties of Pure and Ni-Fe-Codoped Zinc Oxide Nanoparticles Synthesized by a Sol-Gel Autocombustion Method. *ACS Omega*, 2024, *9* (1), 137–145. https://doi.org/10.1021/acsomega.3c01727.

[24] Gamal, H.; Tawfik, Prof. W.; Sayyad, H.; Fahmy, H.; Emam, A.; El-Ghaweet, H. Efficacy of Polyvinylpyrrolidone-Capped Gold Nanorods against 7,12 Dimethylbenz(a)Anthracene-Induced Oviduct and Endometrial Cancers in Albino Rats. *Egyptian Journal of Basic and Applied Sciences*, 2023, *10*, 274–289. https://doi.org/10.1080/2314808X.2023.2185615.

[25] Gamal, H.; Tawfik, W.; El-Sayyad, H. I.; Emam, A. N.; Fahmy, H. M.; El-Ghaweet, H. A. A New Vision of Photothermal Therapy Assisted with Gold Nanorods for the Treatment of Mammary Cancers in Adult Female Rats. *Nanoscale Adv*, 2023, *6* (1), 170–187. https://doi.org/10.1039/d3na00595j.

[26] Gamal, H.; Tawfik, Prof. W.; Fahmy, H.; El-Sayyad, H. Breakthroughs of Using Photodynamic Therapy and Gold Nanoparticles in Cancer Treatment; 2021; pp 1–4. https://doi.org/10.1109/5NANO51638.2021.9491133.

[27] Li, Z.; Lei, H.; Kan, A.; Xie, H.; Yu, W. Photothermal Applications Based on Graphene and Its Derivatives: A State-of-the-Art Review. *Energy*, 2021, *216*, 119262. https://doi.org/https://doi.org/10.1016/j.energy.2020.119262.

[28] M. Nizam, N. U.; Hanafiah, M.; Mahmoudi, E.; Mohammad, A.; Adeleke, A. Effective Adsorptive Removal of Dyes and Heavy Metal Using Graphene Oxide Based Pre-Treated with NaOH / H2SO4 Rubber Seed Shells Synthetic Graphite Precursor: Equilibrium Isotherm, Kinetics and Thermodynamic Studies. *Sep Purif Technol*, 2022, *289*, 120730. https://doi.org/10.1016/j.seppur.2022.120730.

[29] Mamidi, S.; Pandey, A.; Pathak, A.; Rao, T.; Sharma, C. Pencil Lead Powder as a Cost-Effective and High-Performance Graphite-Silica Composite Anode for High Performance Lithium-Ion Batteries. *J Alloys Compd*, 2021, *872*, 159719. https://doi.org/10.1016/j.jallcom.2021.159719.

[30] Chen, J.; Yao, B.; Li, C.; Shi, G. An Improved Hummers Method for Eco-Friendly Synthesis of Graphene Oxide. *Carbon N Y*, 2013, *64*, 225–229. https://doi.org/10.1016/j.carbon.2013.07.055.

[31] Bharali, D. J.; Lucey, D. W.; Jayakumar, H.; Pudavar, H. E.; Prasad, P. N. Folate-Receptor-Mediated Delivery of InP Quantum Dots for Bioimaging Using Confocal and Two-Photon Microscopy. *J Am Chem Soc*, 2005, *127* (32), 11364–11371. https://doi.org/10.1021/ja051455x.

[32] Huang, P.; Xu, C.; Lin, J.; Wang, C.; Wang, X.; Zhang, C.; Zhou, X.; Guo, S.; Cui, D. *Folic Acid-Conjugated Graphene Oxide Loaded with Photosensitizers for Targeting Photodynamic Therapy*; 2011; Vol. 1.

[33] Zhang, C.; Hu, D. F.; Xu, J. W.; Ma, M. Q.; Xing, H.; Yao, K.; Ji, J.; Xu, Z. K. Polyphenol-Assisted Exfoliation of Transition Metal Dichalcogenides into Nanosheets as Photothermal Nanocarriers for Enhanced Antibiofilm Activity. *ACS Nano*, 2018, *12* (12), 12347–12356. https://doi.org/10.1021/acsnano.8b06321.

[34] Ahmed, N.; Ahmed, R.; Rafiqe, M. A Comparative Study of Cu–Ni Alloy Using LIBS, LA-TOF, EDX, and XRF. *Laser and Particle Beams*, 2016, *35*, 1–9. https://doi.org/10.1017/S0263034616000732.

[35] Liu, Y.; Peng, J.; Wang, S.; Xu, M.; Gao, M.; Xia, T.; Weng, J.; Xu, A.; Liu, S. Molybdenum Disulfide/Graphene Oxide Nanocomposites Show Favorable Lung Targeting and Enhanced Drug Loading/Tumor-Killing Efficacy with Improved Biocompatibility. *NPG Asia Mater*, 2018, *10* (1), e458–e458. https://doi.org/10.1038/am.2017.225.

[36] Yogesh, G. K.; Shuaib, E. P.; Roopmani, P.; Gumpu, M. B.; Krishnan, U. M.; Sastikumar, D. Synthesis, Characterization and Bioimaging Application of Laser-Ablated Graphene-Oxide Nanoparticles (NGOs). *Diam Relat Mater*, 2020, *104*. https://doi.org/10.1016/j.diamond.2020.107733.

[37] Lalithambika, K. C.; Shanmugapriya, K.; Sriram, S. Photocatalytic Activity of MoS2 Nanoparticles: An Experimental and DFT Analysis. *Appl Phys A Mater Sci Process*, 2019, *125* (12). https://doi.org/10.1007/s00339-019-3120-9.

[38] Sarwar, S.; Karamat, S.; Saleem Bhatti, A.; Kadri Aydinol, M.; Oral, A.; Hassan, M. U. Synthesis of Graphene-MoS2 Composite Based Anode from Oxides and Their Electrochemical Behavior. *Chem Phys Lett*, 2021, *781*. https://doi.org/10.1016/j.cplett.2021.138969.

[39] Ding, X.; Huang, Y.; Li, S.; Zhang, N.; Wang, J. 3D Architecture Reduced Graphene Oxide-MoS2 Composite: Preparation and Excellent Electromagnetic Wave Absorption Performance. *Compos Part A Appl Sci Manuf*, 2016, *90*, 424–432. https://doi.org/10.1016/j.compositesa.2016.08.006.

[40] Mutalib, T. N. A. B. T. A.; Tan, S. J.; Foo, K. L.; Liew, Y. M.; Heah, C. Y.; Abdullah, M. M. A. B. Properties of Polyaniline/Graphene Oxide (PANI/GO) Composites: Effect of GO Loading. *Polymer Bulletin*, 2021, *78* (9), 4835–4847. https://doi.org/10.1007/s00289-020-03334-w.

[41] Vikraman, D.; Akbar, K.; Hussain, S.; Yoo, G.; Jang, J. Y.; Chun, S. H.; Jung, J.; Park, H. J. Direct Synthesis of Thickness-Tunable MoS2 Quantum Dot Thin Layers: Optical, Structural and Electrical Properties and Their Application to Hydrogen Evolution. *Nano Energy*, 2017, *35*, 101–114. https://doi.org/10.1016/j.nanoen.2017.03.031.

[42] Qin, W.; Chen, T.; Pan, L.; Niu, L.; Hu, B.; Li, D.; Li, J.; Sun, Z. MoS2-Reduced Graphene Oxide Composites via Microwave Assisted Synthesis for Sodium Ion Battery Anode with Improved Capacity and Cycling Performance. *Electrochim Acta*, 2015, *153*, 55–61. https://doi.org/10.1016/j.electacta.2014.11.034.

[43] Zhang, T.; Zhu, G.-Y.; Yu, C.-H.; Xie, Y.; Xia, M.-Y.; Lu, B.-Y.; Fei, X.; Peng, Q. The UV Absorption of Graphene Oxide Is Size-Dependent: Possible Calibration Pitfalls. *Microchimica Acta*, 2019, *186* (3), 207. https://doi.org/10.1007/s00604-019-3329-5.

[44] Matias, R.; Ribeiro, P. R. S.; Sarraguça, M. C.; Lopes, J. A. A UV Spectrophotometric Method for the Determination of Folic Acid in Pharmaceutical Tablets and Dissolution Tests. *Analytical Methods*, 2014, *6* (9), 3065–3071. https://doi.org/10.1039/c3ay41874j.

[45] KEKLİKCİOĞLU ÇAKMAK, N.; KÜÇÜKYAZICI, M.; EROĞLU, A. Synthesis and Stability Analysis of Folic Acid-Graphene Oxide Nanoparticles for Drug Delivery and Targeted Cancer Therapies. *International Advanced Researches and Engineering Journal*, 2019, *3* (2), 81–85. https://doi.org/10.35860/iarej.411717.

[46] Hu, Z.; Li, J.; Li, C.; Zhao, S.; Li, N.; Wang, Y.; Wei, F.; Chen, L.; Huang, Y. Folic Acid-Conjugated Graphene-ZnO Nanohybrid for Targeting Photodynamic Therapy under Visible Light Irradiation. *J Mater Chem B*, 2013, *1* (38), 5003–5013. https://doi.org/10.1039/c3tb20849d.

[47] Khalili, D. Graphene Oxide: A Promising Carbocatalyst for the Regioselective Thiocyanation of Aromatic Amines, Phenols, Anisols and Enolizable Ketones by Hydrogen Peroxide/KSCN in Water. *New J. Chem.*, 2016, *40* (3), 2547–2553. https://doi.org/10.1039/C5NJ02314A.

[48] Song, H.; Wang, B.; Zhou, Q.; Xiao, J.; Jia, X. Preparation and Tribological Properties of MoS 2 /Graphene Oxide Composites. *Appl Surf Sci*, 2017, *419*, 24–34. https://doi.org/10.1016/j.apsusc.2017.05.022.

[49] Liu, R.; Wang, H.; Yue, C.; Zhang, X.; Wang, M.; Liu, L. Synthesis of Molybdenum Disulfide/Graphene Oxide Composites for Effective Removal of U (VI) from Aqueous Solutions. *J Radioanal Nucl Chem*, 2022, *331* (9), 3713–3722. https://doi.org/10.1007/s10967-022-08425-8.

[50] Muhammad, N.; Sarfraz, Z.; Zafar, M. S.; Liaqat, S.; Rahim, A.; Ahmad, P.; Alsubaie, A.; Almalki, A. S. A.; Khandaker, M. U. Characterization of Various Acrylate Based Artificial Teeth for Denture Fabrication. *J Mater Sci Mater Med*, 2022, *33* (2). https://doi.org/10.1007/s10856-022-06645-8.

[51] Elshafie, M.; Taha, M. G.; Elhamamsy, S. M.; Moustafa, Y.; Elazab, W. I. M. Thermal Analysis of the Prepared Lignin/Graphene Oxide/Polyurethane Composite. *Egyptian Journal of Petroleum*, 2020, *29* (2), 195–201. https://doi.org/https://doi.org/10.1016/j.ejpe.2020.04.001.

[52] Thangappan, R.; Kalaiselvam, S.; Elayaperumal, A.; Jayavel, R.; Arivanandhan, M.; Karthikeyan, R.; Hayakawa, Y. Graphene Decorated with MoS2 Nanosheets: A Synergetic Energy Storage Composite Electrode for Supercapacitor Applications. *Dalton Transactions*, 2016, *45* (6), 2637–2646. https://doi.org/10.1039/c5dt04832j.

[53] Song, M.; Yu, L.; Wu, Y. Simple Synthesis and Enhanced Performance of Graphene Oxide-Gold Composites. *J Nanomater*, 2012, *2012*. https://doi.org/10.1155/2012/135138.

[54] Adel, M.; El-Maghraby, A.; El-Shazly, O.; El-Wahidy, E. W. F.; Mohamed, M. A. A. Production of Reduced Graphene Oxide from Glucose via Hydrothermal Route: The Crucial Role of the Evolved Byproduct Gases in Deoxygenating the Graphitic Structure. *J Mater Res*, 2021, *36* (4), 896–905. https://doi.org/10.1557/s43578-020-00039-8.